HHS Public Access

Author manuscript

Hum Mutat. Author manuscript; available in PMC 2020 July 01.

Published in final edited form as:

Hum Mutat. 2019 July ; 40(7): 983–995. doi:10.1002/humu.23758.

Functional and Structural Analysis of Rare *SLC2A2* Variants Associated with Fanconi-Bickel Syndrome and Metabolic Traits

Osatohanmwen J. Enogieru[1], **Peter M.U. Ung**[2], **Sook Wah Yee**[1], **Avner Schlessinger**[2], **Kathleen M. Giacomini**[1,3]

[1]Department of Bioengineering and Therapeutic Sciences, University of California, San Francisco, San Francisco, California, 94158 United States

[2]Department of Pharmacological Sciences, Icahn School of Medicine at Mount Sinai, New York, New York 10029, United States

[3]Institute for Human Genetics, University of California, San Francisco, San Francisco, California, 94158 United States

Abstract

Deleterious variants in *SLC2A2* cause Fanconi-Bickel Syndrome (FBS), a glycogen storage disorder, whereas less common variants in *SLC2A2* associate with numerous metabolic diseases. Phenotypic heterogeneity in FBS has been observed, but its causes remain unknown. Our goal was to functionally characterize rare *SLC2A2* variants found in FBS and metabolic disease-associated variants to understand the impact of these variants on GLUT2 activity and expression, and establish genotype-phenotype correlations.

cRNA-injected *Xenopus laevis* oocytes were used to study mutant transporter activity and membrane expression. GLUT2 homology models were constructed for mutation analysis using GLUT1, GLUT3 and XylE as templates.

Seventeen FBS variants were characterized. Only c.457_462delCTTATA (p.Leu153_Ile154del) exhibited residual glucose uptake. Functional characterization revealed that only half of the variants were expressed on the plasma membrane. Most less common variants (except c.593C>A (p.Thr198Lys) and c.1087G>T (p.Ala363Ser)) exhibited similar GLUT2 transport activity as the

The corresponding author is Kathleen M. Giacomini: Department of Bioengineering and Therapeutic Sciences, UCSF Rock Hall Box 2911, 1550 4th Street RH 581, San Francisco, CA 94158, Telephone number: (415) 476-1936; Fax number: (415) 514-4361, Kathy.Giacomini@ucsf.edu.

Author's contributions

OJE, SWY and KMG designed the study, analyzed and interpreted the data. OJE assembled and cataloged all published FBS case reports. SWY and OJE selected variants associated with metabolic traits. OJE conducted the uptake, expression and kinetic assays while PMUU and AS constructed the computational model and conducted structural analysis and simulations. OJE, SWE and KMG wrote the majority of the paper; PMUU wrote the structural analysis (methods, results) portion of the paper with guidance from AS. All authors read and approved the final manuscript.

Conflict of Interest statement

None declared.

Ethical Compliance

This manuscript uses and references retrospective case report data, which does not require ethics committee approval at the University of California San Francisco (UCSF). Ecocyte Bio Science LLC is approved by the Institutional Animal Care and Use Committee (IACUC); their Xenopus laevis frog maintenance and surgical procedures follow the IACUC guidelines. According to UCSF's IACUC program, the research conducted in our study is exempt from IACUC approval. All de-identified human genetic variant data were derived from the Type 2 diabetes knowledge portal, 1000 Genomes Browser, gnomAD browser and published case reports.

wild-type. Structural analysis of GLUT2 revealed that variants affect substrate-binding, steric hindrance, or overall transporter structure.

The mutant transporter that is associated with a milder FBS phenotype, p.Leu153_Ile154del, retained transport activity. These results improve our overall understanding of the underlying causes of FBS and impact of GLUT2 function on various clinical phenotypes ranging from rare to common disease.

Keywords

glucose transport; Fanconi-Bickel syndrome; GLUT2; *SLC2A2*; rare variants; rare disease; orphan disease; glycogen storage; structural homology; Type 2 Diabetes

INTRODUCTION

Pathogenic variants in *SLC2A2*, the gene that encodes for the glucose transporter, GLUT2, have been associated with Fanconi-Bickel Syndrome (FBS; MIM# 227810), a rare glycogen storage disorder that has over 100 documented cases published (Santer et al., 1997, Santer et al., 2002). These deleterious, rare variants (minor allele frequency < 1%) effectively abolish GLUT2 transporter function, which leads to significant physiological sequelae. Currently, forty-six *SLC2A2* variants have been identified and associated with FBS; these include missense, nonsense, in-frame indels (insertions/deletions), frame-shift indels and splice site variants. FBS is an autosomal recessive disease; in order for FBS to manifest in an individual, the person must be homozygous or compound heterozygous with two pathogenic *SLC2A2* variants. Figure 1 displays the location of many of the GLUT2 variants that are causal for FBS; these variants are scattered throughout GLUT2.

Common signs and symptoms of the syndrome include hepatomegaly, stunted growth and rickets due to renal losses of calcium and phosphate, high postprandial and low pre-prandial blood glucose levels. These typical manifestations are directly related to the tissue specificity of GLUT2 transporters (liver, kidney, intestine, and to a lesser extent pancreatic beta cells) (Mueckler & Thorens, 2013). As the primary glucose transporter in hepatocytes, GLUT2 regulates the normal flow of glucose to and from the liver, and its loss leads to excessive glycogen storage (hepatomegaly). In the kidney, GLUT2 is located in the proximal tubule and is involved in the reabsorption of glucose from urine into the blood. The absence of GLUT2 in the kidney causes massive glucosuria plus significant loss of minerals required for bone growth and strength (calcium, phosphate) leading to bone deformities (Santer et al., 1998). However, as with many diseases, FBS presents with a spectrum of phenotypes. Whereas some patients develop severe symptoms that are recalcitrant to treatment such as bone fractures (Berry et al., 1995; Manz et al., 1987), hepatocellular carcinoma (Pogoriler et al., 2017), liver failure and premature death (Karamizadeh et al., 2012; Yoo et al., 2002), others present with a “milder” clinical picture (relatively normal growth, no hepatomegaly, minor kidney dysfunction) that can be corrected with conservative measures (Grünert et al., 2012).

Although GLUT2 variants associated with published cases of FBS have been identified, the majority have not been evaluated for their impact on GLUT2 function. To date, only five FBS variants have been functionally characterized (c.724A>C, p.Ser242Arg; c.1330T>C, p.Trp444Arg; c.1250C>T, p.Pro417Leu; c.59G>A, p.Gly20Asp; c.372A>C, p.Arg124Ser) (Mannstadt et al., 2012, Michau et al., 2013). Furthermore, the relationship between the functional effects of any of the mutant transporters and the phenotypic presentation of the disease has not been established. Since 2000, many new cases of FBS from around the world have been identified revealing a host of novel variants, but these new variants have not been functionally evaluated or characterized (Abbasi et al., 2015; Amita et al., 2017; Bahíllo-Curieses et al., 2017; Grünert et al., 2012; Hadipour et al., 2013; Odièvre et al., 2002; Peduto et al., 2004; Pogoriler et al., 2017; Su et al., 2011; Wang et al., 2015). Cases of heterozygote carriers of FBS variants, i.e. parents or siblings of FBS patients, that experience glycemic perturbations (i.e. glycosuria, impaired glucose tolerance) have been documented (Sakamoto et al., 2000). Sakamoto and colleagues hypothesized that GLUT2 proteins could exhibit a dominant negative effect (i.e. haploinsufficiency) in individuals heterozygous with an FBS GLUT2 missense variant.

In addition to individuals who are homozygous for rare, deleterious variants in GLUT2 that are causal for FBS, those who harbor at least one less common (minor allele frequency between 1 – 5%) or common (minor allele frequency > 5%) *SLC2A2* allele may be at risk for various metabolic traits. For example, genome-wide association studies (GWAS) have identified common and less common variants in *SLC2A2* that associate with an increased risk of Type 2 diabetes (T2D) (Scott et al., 2017), as well as increases in fasting glucose (Dupuis et al., 2010, Manning et al., 2012), glycated hemoglobin levels (HbA1c) (Barker et al., 011, Wheeler et al., 2017) and even differential response to metformin (Zhou K et al., 2016). Furthermore, several less common *SLC2A2* variants that are only found in specific populations significantly associate with increased risk of T2D, elevated blood glucose, and cholesterol levels and other metabolic perturbations (Type 2 Diabetes Knowledge Portal: http://www.type2diabetesgenetics.org).

In this study, we performed detailed functional analyses of all reported, but uncharacterized missense and in-frame indel FBS variants, as well as less common variants that associate with metabolic perturbations. In order to determine the impact of these variants on GLUT2 transporter function, our studies focused on assessing the function of mutant or polymorphic transporters, as well as plasma membrane expression. A GLUT2 homology model was used to propose the molecular mechanisms by which particular FBS variants cause GLUT2 structural instability and abrogate GLUT2 transporter function. Overall, this study creates a comprehensive catalog of the functional characteristics of all reported missense and in-frame indel variants associated with FBS and metabolic perturbations, along with a GLUT2 structure-function map. *In vitro* function for some of the GLUT2 variants is related to clinical phenotypic characteristics suggesting that understanding the functional effects of variants in GLUT2 may help explain the phenotypic heterogeneity within the FBS patient population, as well as the influence of *SLC2A2* polymorphisms on metabolic traits.

RESULTS

-FBS is rare yet reported throughout the world in every major ethnic group

We collected information on over 70 patients with FBS including the patient's genotype, demographic characteristics, and available clinical information (Supp. Table S1). The demographic information in Supp. Table S1 shows that FBS has been reported in every major human ethnic group. The first case of FBS was reported in Switzerland in 1949 (Fanconi & Bickel, 1949); the first Chinese patients diagnosed with FBS was in 2011 (Su et al., 2011); and the first African-American patient diagnosed with FBS was in 2016 (Gupta et al., 2016). Our updated FBS case list includes more than ten novel amino acid variants that were published after the last published FBS review in 2002 (Santer et al., 2002). These novel variants plus other FBS variants are scattered throughout the transporter, from the first transmembrane (TM) helix (e.g. c.59_60delinsAA, p.Gly20Glu) to the start of the carboxyl terminal tail (e.g. c.1439C>G; p.Thr480Arg) (Figure 1). PhyloP scores measure evolutionary conservation at individual alignment sites expected under neutral drift (Pollard et al., 2010); positive scores indicate sites that are predicted to be conserved while negative scores indicate sites that are predicted to be fast-evolving. With few exceptions, most of the FBS *SLC2A2* variants occur in areas that are highly conserved amongst one hundred vertebrate species (PhyloP scores ≥ 2) and highly conserved amongst GLUT1 to GLUT5 transporters (Supp. Table S2, Supp. Figure S1) (Pollard et al., 2010; Waterhouse et al., 2009).

The SNP annotation scores of the five SLC2A2 missense variants associated with metabolic traits

Five previously uncharacterized missense variants in *SLC2A2* that have significant associations with metabolic traits were found to have allele frequencies between 0.1–5% in certain ethnic populations (Supp. Table S3). Amongst these variants, Polyphen-2 (Adzhubei et al., 2010) predicted that one was probably damaging (c.301G>A, p.Val101Ile), two were possibly damaging (c.593C>A, p.Thr198Lys and c.1087G>T, p.Ala363Ser), and two were benign (c.1402C>G, p.Leu468Val, c.1556G>A, p.Gly519Glu). Among the three variants predicted to be probably or possibly damaging, two of them, p.Val101Ile and p.Ala363Ser, are conserved (PhyloP score > 2 and GERP score > 4). Interestingly, p.Val101Ile is predicted by various prediction scores to be damaging or deleterious (Polyphen-2, SIFT (Ng et al., 2003), CADD (Kircher et al., 2014), GERP (Cooper et al., 2005)) and predicted by REVEL (Ioannidis et al., 2016) to be partially damaging (score 0.46 (range from 0 to 1.0)) (Supp. Table S3). In addition, valine in position 101 is conserved across human GLUT1 to GLUT5 (Supp. Figure S1) (Waterhouse et al., 2009).

Functional characterization of seventeen FBS mutations in oocytes reveals a mutant transporter with residual function

All of the FBS mutant transporters had significantly reduced uptake of substrate compared with wild-type GLUT2 (Figure 2, one-way ANOVA $F = 467.7$; p-value < 0.0001). The uptake rate of 2DG (2-deoxy-glucose) by most FBS mutant transporters was comparable to that of saline-injected oocytes. With the exception of one mutant (c.457_462delCTTATA, p.Leu153_Ile154del), all FBS mutants exhibited effectively no transport function, with uptake rates measured to be on average approximately 0.5 pmol/0.5hr/oocyte (Figure 2).

Remarkably, p.Leu153_Ile154del still exhibited residual uptake of 2DG (2.174 pmol/0.5hr/oocyte), which was significantly higher than the other FBS mutants (one-way ANOVA F = 5.591, *p-value = 0.0006) but still much lower than wild-type GLUT2 (student's t-test 37.16 ± 1.1 vs. 2.174 ± 0.23 pmol/0.5hr/oocyte; p-value < 0.0001). Nine of the seventeen evaluated FBS mutant transporters were expressed on the plasma membrane and had similar expression to wild-type GLUT2 (one-way ANOVA F-value = 0.6534; p-value = 0.74). The other eight mutants had partial or negligible plasma membrane expression compared to wild-type GLUT2 (one-way ANOVA F-value = 23.05; p-value < 0.0001, Supp. Table S2).

Functional characterization of five missense variants in SLC2A2, associated with metabolic traits reveals mutations with partial function

We characterized five missense variants that were associated with metabolic traits (Supp. Table S3). Three out of the five transporters had transport rates (one-way ANOVA F-value = 0.115, p-value = 0.95) statistically comparable to wild-type GLUT2 (Figure 3). p.Thr198Lys exhibited a partially reduced transport rate; it retained approximately 50% (23 pmol/0.5hr/oocyte) of transport activity compared to the wild-type (39.2 pmol0.5hr/oocyte, student's t-test, **p-value = 0.005). The rate of 2DG uptake by p.Ala363Ser was similar to that of saline-injected oocytes (0.42 pmol/0.5hr/oocyte).

Except for p.Ala363Ser, all of the above mutants were expressed on the oocyte plasma membrane (one-way ANOVA F-value = 0.3502, p-value = 0.88) in a manner comparable to wild-type GLUT2. The estimated K_m values of all mutant transporters associated with metabolic traits were not statistically different from that of wild-type GLUT2 (Figure 4, Table 1; one way ANOVA, p-value = 0.44). Similarly, the estimated V_{max} values of all mutant transporters were not statistically different from that of wild-type GLUT2 (one-way ANOVA, p-value = 0.48) with the exception of p.Thr198Lys, which had a V_{max} value much lower than the wild-type GLUT2 transporter (11±1.7 vs 53±2.0 nmol/0.5hr/oocyte, student's t-test ***p-value = 0.0044). Michaelis-Menten curves could not be generated for p.Ala363Ser (signal undetectable in oocytes).

Functional characterization of GLUT2 mutant transporters in mammalian cells

The maximum increase in 2DG uptake in Flp-In™ 293 cells expressing full-length wild-type GLUT2 and empty vector was approximately 50–80% (data not shown). To improve the signal-to-noise ratio, the uptake of radiolabeled fructose was tested. The fold difference in fructose uptake between pcDNA5-EV cells and pcDNA5-GLUT2 cells was approximately 2× (Supp. Figure S2). The improvement in signal-to-noise ratio with fructose is due to its increased selectivity for GLUT2 compared to human GLUT1, GLUT3, and GLUT4 transporters that are present in immortalized mammalian cell lines (Seatter et al., 1998). Therefore, [^{3}H]-fructose (fructose 100μM total concentration) was used as the radiolabeled substrate for the following Flp-In™ 293 radiolabeled substrate uptake experiments.

As expected, the cells transfected with pcDNA5-GLUT2 FBS mutants had fructose uptake values similar to cells transfected with empty vector (Supp. Figure S2, one-way ANOVA, F=1.218, p-value = 0.2989). In contrast, fructose uptake was similar in cells transfected with mutants associated with metabolic traits (p.Val101Ile, p.Ala363Ser, p.Leu468Val,

p.Gly519Glu) and cells transfected with full-length wild-type GLUT2 (one-way ANOVA, F=1.693, p-value = 0.1558), except for p.Thr198Lys. Fructose uptake rate in cells expressing p.Thr198Lys was slightly lower than in cells expressing wild-type GLUT2, though higher than in cells transfected with empty vector (Student's t-test p-value <0.0001). The results in mammalian cells exhibited a similar trend with the results in the oocytes, except for p.Ala363Ser. Unexpectedly, we found that p.Ala363Ser transporter, which was not expressed on the plasma membrane of *X. laevis* oocytes (Figure 3), was expressed well in Flp-In™ 293 cells and transported fructose at a similar rate as wild-type GLUT2 (Supp. Figure S2). Interestingly, inhibition of the proteasome in oocytes led to increased expression of p.Ala363Ser transporter on the plasma membrane and had a similar activity as wild-type GLUT2 (Supp. Figure S3). Discrepancies between heterologously expressed transporter activity in oocytes versus HEK293 cells have been previously observed. For example, Karniski and colleagues found that two out of the six variants in the sulfate transporter (DTDST) that were previously considered "partial activity" transporters in oocytes (Karniski et al., 2001) demonstrated no activity in Flp-In™ 293 cells (Karniski et al., 2004).

Temperature-sensitive mutants may also function differently in oocytes (generally studied between 25–30°C and mammalian cells which are usually studied at 37°C (Baron et al., 2002, Machamer et al.,1988, Woodward et al., 2013). We determined that p.Ala363Ser is probably not temperature-sensitive because p.Ala363Ser transport function was similar to wild-type GLUT2 at 37°C (Flp-In™ 293 cells, Supp. Figure S2) and 18°C (oocytes plus proteasome inhibitor, Supp. Figure S3). Our result showed that proteasome inhibition in Flp-In™ 293 cells does not change the transport function of p.Ala363Ser (Supp. Figure S4), which suggests that the proteasome machinery of *Xenopus laevis* oocytes differs from HEK293 cells

The frequency of FBS SLC2A2 alleles in the population

Among the 17 FBS mutations characterized in this study, six were reported in various sequencing databases (c.115_117delATA, p.Ile39del; c.380C>A, p.Ala127Asp; p.Leu153_Ile154del; c.952G>A, p.Gly318Arg; p.Pro417Leu and c.1250C>G, p.Pro417Arg) like the gnomAD and Geno2MP browsers, (Geno2MP: http://geno2mp.gs.washington.edu/Geno2MP/#/; Lek et al., 2016). Neither database reported a homozygote carrier of the six variants. Most of these variants have one to three allele counts, except for, p.Ile39del and p.Leu153_Ile154del which were more common (i.e. 8 and 22 allele counts, respectively, in gnomAD; 3 alleles of p.Leu153_Ile154del reported in Geno2MP).

Structural analysis proposes molecular mechanisms of GLUT2 transporter dysfunction

SLC2A2 variants associated with FBS or metabolic traits that were expressed on the plasma membrane were selected for structural analysis. The structure of GLUT2 is currently unknown, however, structures of other human *SLC2* members as well as the closely related prokaryotic homolog XylE, have been determined in atomic resolution, providing excellent templates to model GLUT2 (Colas et al., 2016). We therefore generated homology models of GLUT2 in three different conformations to analyze the variants (Figure 5a). While the majority of these FBS variants occurred in the TM helices away from the substrate-binding site (> 5Å), we speculate that these variants affected function through altered packing of the

TM helices or protein dynamics. The predicted effects of seven variants on the molecular attributes of GLUT2 that are needed for transport are described below (predictions of other variants are described in Supp. Table S4). c.96T>G, p.Asn32Lys and c.976_977delinsAA, p.Ser326Lys both lie in the extracellular channel of the transporter in TM1 and TM7, respectively. Their charged, bulky guanidinium side chain can sterically hinder the passage of the substrate through the channel (Figure 5b, Supp. Movie S1 and Supp. Movie S2). c.609T>A, p.Ser203Arg is positioned on TM5; the variant introduces large steric clashes and electrostatic repulsion that alter the packing of TM5 and TM1 and influence TM1 dynamics. Furthermore, the basic, guanidinium side chain may reach into the substrate-binding site, directly affecting substrate binding (Supp. Movie S3).

p.Gly318Arg, which is located next to substrate-binding site (Figure 5c), significantly influences the helix bending of TM7 while its large steric bulk affects the helix packing. These structural effects may alter the equilibrium of the conformation ensemble of the transporter and favour the inward-open conformation, resulting in the substrate being excluded from the substrate-binding site (Supp. Movie S4).

c.1246G>A, p.Gly416Ser is a variant along the transporter's channel and can interact with the substrate. It is a variant on TM10 and in the critical (GPGPXP) helix kink formation, which can affect the helix packing and TM10 bending. In addition, p.Gly416Ser can directly interact with the binding site residues Glu412, and Gln193 on TM5, thus directly affecting binding site shape and biophysical properties (Supp. Movie S5).

p.Pro417Leu, a commonly reported FBS variant, was functionally characterized previously and shown to be expressed on the plasma membrane (Michau et al., 2013).

According to our analysis, p.Pro417Leu directly and indirectly impacts several substrate-binding residues (Figure 5d). Specifically, p.Pro417Leu loses the backbone amide hydrogen bond to the *i+4* residue (von Heijne et al., 1991) and distorts the natural (GPGPXP) helix kink formation, which can lead to the indole sidechain of p.Trp420 to twist away and prevent interaction with the substrate (Supp. Movie S6). This variant introduces large steric bulk affecting the tight helix packing, resulting in the distortion of binding site residues (p.Glu412, p.Asn349, and p.Gln193).

Another variant at position 417, p.Pro417Arg, also affects the kink of helix. Both p.Pro417Leu and p.Pro417Arg have the steric bulk that can affect the helix packing in the region (Figure 5d). But p.Pro417Arg establishes an extensive hydrogen bond network with the surrounding residues and helices that potentially limits the expulsion movement of the other helices (Supp. Movie S7). p.Pro417Leu does not have this hydrogen bond network, and its steric bulk will expel the other packing helices.

DISCUSSION

In this study, we performed a comprehensive functional characterization of seventeen *SLC2A2* missense and in-frame indel mutant transporters associated with a range of FBS phenotypes and five *SLC2A2* missense variants associated with various metabolic perturbations (e.g. T2D, elevated HbA1c concentration, increased fasting glucose levels).

Previously, only five FBS mutant transporters had been characterized out of over 40 known variants and to our knowledge, only three *SLC2A2* missense variants associated with metabolic traits have been characterized (c.329C>T, p.Thr110Ile; c.203C>T, p.Pro68Leu and c.589G>A, p.Val197Ile (Supp. Table S3, Supp. Figure S5) (Abbasi et al., 2015; Amita et al., 2017; Gupta et al., 2016; Michau et al., 2013; Pogoriler et al., 2017; Wang et al., 2015). Generally, in order for FBS to manifest in an individual, the person must be homozygous or compound heterozygous with two deleterious *SLC2A2* variants. The functional and structural evaluation of these variants led to four major findings. First, variants associated with FBS virtually abolished transport function; however, one variant, p.Leu153_Ile154del, found in two cases of mild FBS, exhibited residual transport function. Second, about half of the FBS mutant transporters were not expressed (or expressed at low levels) on the plasma membrane, whereas the other half were expressed on the membrane but exhibited no transport activity. Third, structural analysis provided a mechanistic rationale for the deleterious effects of GLUT2 genetic variants that were expressed on the plasma membrane. Fourth, two less common variants, p.Thr198Lys and p.Ala363Ser, which are associated with increased glycated hemoglobin levels and T2D, exhibited reduced activity in oocytes. Below we discuss each of these findings in the context of the literature.

First, of the seventeen variants in GLUT2 that had not previously been characterized, all but one (p.Leu153_Ile154del) abolished transport function. To the best of our knowledge, p.Leu153_Ile154del is the first *SLC2A2* variant associated with FBS that results in a GLUT2 that retains some function, albeit minimal. The patients documented with a mild form of FBS were compound heterozygotes for the variants, p.Leu153_Ile154del and p.Pro417Arg. Our data show that p.Pro417Arg has no activity. Though speculative, the data suggest that the residual activity of p.Leu153_Ile154del transporter was sufficient to rescue the severe phenotype commonly associated with FBS, resulting in a milder phenotype. The data may suggest that the meager function of one GLUT2 allele can significantly mitigate the most severe signs and symptoms of FBS. This has been demonstrated in other rare genetic diseases in which variants that result in partially active enzymes, transporters or channels are associated with a mild to moderate form of the disease and variants that result in non-functional enzymes, transporters or channels lead to the most severe forms (e.g. DTDST variants and chrondrodysplasias) (Karniski et al., 2001, Karniski et al., 2004).

Second, the loss of function of about half of the mutant GLUT2 transporters was due to lack of expression on the plasma membrane. Various mechanisms for improper sorting of mutant transporters in GLUTs and other *SLC*s have been described (El-Kasaby et al., 2014; Koban et al., 2015; Skach et al., 2000, Toye et al., 2005; Wieman et al., 2009). Generally, these mechanisms involve the retention (in ER or Golgi apparatus) and eventual destruction of aggregated or misfolded mutant protein or the misdirection of mutant protein to the incorrect membrane (Asjad et al., 2017; El-Kasaby et al., 2014; Koban et al., 2015; Skach et al., 2000; Toye et al., 2005).

GLUT1, GLUT3 and GLUT4 have known sorting sequences, DSQV (Wieman et al., 2009), DRSGKDGVMEMN (Inukai et al., 2004), and FQQI, TELEY, LL (Blot et al., 2008), respectively, that localize these GLUTs to their extracellular or intracellular membrane compartments. GLUT1 variants that occur near phosphorylation motifs that enhance

membrane localization have been shown to reduce or prevent membrane expression of transporters, leading to GLUT1 deficiency syndromes (Lee et al., 2015). MetaServer, a tool that predicts peptide binding sequences within proteins, predicted several sequences in GLUT2 that could bind to proteins that regulate membrane trafficking (Kundu & Backofen, 2014; Kundu, Costa, & Backofen, 2013; Kundu, Costa, Huber, Reth, & Backofen, 2013; Kundu, Mann, Costa, & Backofen, 2014).

Of the 18 sequence-motifs in GLUT2 predicted to harbor binding sites for proteins that regulate trafficking, one is changed by an FBS variant characterized in our study (c.715_717delTGT, p.239delCys; Supp. Figure S6). Consistently, p.239delCys was not expressed on the plasma membrane. However, because these predicted motifs have not been validated *in vitro*, further work is needed to characterize the regulatory proteins and mechanisms by which these mutants alter plasma membrane expression of GLUT2.

Our third finding was that many variants associated with FBS (nine out of the seventeen FBS mutant transporters) result in expression levels on the plasma membrane that are comparable to levels of the wild-type GLUT2. Computational analysis of seven out of the nine expressed FBS variants revealed several potential mechanisms by which FBS variants may disrupt transporter activity: steric hindrance of substrate channel (e.g. p.Asn32Lys and p.Ser326Lys), distortion of substrate-binding residues (e.g. p.Ser203Arg, p.Gly416Ser), and instability of TM helices and the overall transporter structure (e.g. p.Gly20Glu, Supp. Table S4). These findings expand on previous findings of structural analysis of pathogenic *SLC2A1* variants that result in GLUT1 deficiency, which suggest that the vast majority of pathological GLUT1 disrupt helix-helix interactions and lead to structural instability of the transporter (Raja & Kinne, 2015). For instance, variants located at or near the substrate channel pathway in GLUT1 have been found to destabilize TM helix-helix interactions and helix packing (e.g. NM_006516.2:c.197C>T, p.Ser66Phe; NM_006516.2:c.929C>T, p.Thr310Ile) (Raja & Kinne, 2015) whereas our analysis showed rare GLUT2 variants that reside on either side of the substrate entrance (e.g. p.Asn32Lys and p.Ser326Lys; Figure 1, Figure 5) block the translocation pathway via their bulky, polar side chains. Similarly, p.Gly318Arg, which is located next to GLUT2 substrate-binding residues, affected TM7 helix bending and packing via it large steric bulk resulting in conformational inflexibility. Only one pathogenic GLUT1 variant directly impacted sugar-interacting residues (1 of 7) (Raja & Kinne, 2015), whereas three of the nine FBS variants evaluated affected substrate-binding residues in GLUT2. For GLUT1, a series of engineered variant in the Ile168 residue, located next to the hinge residue Gly167, which is adjacent to the sugar-binding site, abolished GLUT1 function via increased rigidity and steric hindrance (Ung et al., 2016). Future studies are needed to confirm the mechanisms predicted by the structural model for each of the GLUT2 variants. Overall, these findings suggest that the majority of pathogenic *SLC2* variants disrupt proper packing and dynamics of the TM helices or affect the shape and biophysical properties of the substrate binding site, which in turn leads to ineffective transport.

Our final finding, which was not unexpected, was that most of the less common variants that had not been associated with FBS showed similar function to the reference GLUT2 (Figure 3, Supp. Table S3). These variants, most of which retained normal GLUT2 transport activity,

have been associated, but at weak p-values, with various metabolic traits (e.g. T2D, high body mass index). The minor allele of p.Val101Ile and p.Gly519Glu are on the same haplotype with the reference allele (T) of rs8192675, a known eQTL (expression quantitative trait locus) that associates with increased risk of T2D (Supp. Figure S7) (Machiela & Chanock, 2018). The minor allele of p.Leu468Val, which is associated with increased risk of T2D (OR=1.75, p=0.017) and fasting glucose (beta=0.58, p=0.003) is on the same haplotype with the reference G-allele of p.Thr110Ile, which itself has been associated with increased risk of T2D and fasting glucose (Supp. Table S3, Supp. Figure S7). Structural analysis revealed that p.Thr198Lys (MAF < 0.5%), which displayed reduced substrate uptake in oocytes and Flp-In™ 293 cells (Figure 4, Table 1, Supp. Figure S2), may restrict helix movement and cause disturbance to the protein-lipid interface because of the charged lysine (Supp. Table S4, Supp. Movie S8). This, along with a large reduction in glucose transport capacity (V_{max}), may explain the statistical associations of p.Thr198Lys with increased hemoglobin A1c levels (p=0.012, Supp. Table S3).

One limitation of our study was that we observed differential protein expression of p.Ala363Ser between *X. laevis* oocytes and mammalian cells (Flp-In™ 293 cells) (Supp. Figure S3, Supp. Figure S4, Supp. Movie S9). Normally, expression patterns of heterologously expressed proteins are similar in *Xenopus laevis* oocytes and mammalian cells (Sigel, 1990), but clear examples of differences in the expression of heterologous proteins between cell lines have been reported (Baroudi et al., 2000; Baroudi et al., 2001; Denning et al., 1992; Karniski et al., 2001; Karniski et al., 2004; Machamer & Rose, 1988; Skach et al., 2000; Woodward et al., 2013). Therefore, extrapolation of these data to mammalian cells should be done with caution. The rest of the characterized GLUT2 mutants exhibited the same pattern of transport activity in Flp-In™ 293 cells as they did in *X. laevis* oocytes (Supp. Figure S2).

Conclusions

This comprehensive characterization of variants associated with FBS reveals that about half of the mutant transporters are expressed on the plasma membrane but do not function, and the other half are not significantly expressed on the plasma membrane. Further, we report for the first time that the in-frame deletion variant, p.Leu153_Ile154del, has residual glucose uptake. In contrast, the majority of the five *SLC2A2* missense variants associated with metabolic traits have normal glucose uptake and are expressed on the plasma membrane. The structural analysis corroborates the functional studies and provides mechanistic insights into how these low frequency variants inactivate or reduce GLUT2 transporter activity. The functional and structural information gained in this study suggest that different strategies should be used to produce targeted, safe and effective therapies for FBS and possibly other hGLUT-related diseases.

MATERIALS AND METHODS

-Mutation selection for functional and structural analysis

The approach for variant selection was divided into two categories: variants associated with FBS and variants associated with common metabolic traits. Published FBS case reports, case

series and reviews were acquired via PubMed and various databases. Information on each FBS patient such as demographics, clinical signs and symptoms and genotype, if available, was collected. Cases that did not have clinical data or did not validate clinical FBS diagnosis with a genotype were excluded (approximately twenty cases). The compiled list of variants and associated phenotypes is available (87 cases, Supp. Table S1). We used the Type 2 Diabetes knowledge portal to only select missense variants associated with metabolic traits (e.g. T2D, HbA1c, fasting glucose, fasting insulin and body mass index; p-value < 0.05). Then we used 1000 Genomes Browser and gnomAD browser to determine the allele frequency of the variants in each population (1000 Genomes Consortium, 2015). Based on this criteria, we selected five *SLC2A2* variants that are rare in the general population, but found in less common frequencies in specific populations and ethnicities.

-Mutant plasmid generation using site-directed mutagenesis

For *X. laevis* oocyte studies, site-directed mutagenesis service, performed by GenScript®, was used to create 4 FBS in-frame deletions, 13 FBS missense, and 5 less common missense variants in the human GLUT2 expression vector (pSP64T-GLUT2) provided by Dr. Graeme I. Bell (University of Chicago) (Supp. Table S2, Supp. Table S3). All capped cRNA (wild-type and mutant GLUT2) were synthesized *in vitro* from each respective pSP64T-GLUT2 plasmid using the mMessage mMachine SP6 kit (Thermo Fisher Scientific).

For studies in mammalian cells, GLUT2 cDNA (RefSeq NM_000340.1, NP_000331.1) was cloned into the pcDNA5™/FRT mammalian expression vector (Thermo Fisher Scientific) to produce the pcDNA5-GLUT2 plasmid. Site-directed mutagenesis service, performed by GenScript®, was used to introduce the previously mentioned variants into the expression vector (pcDNA5) (Supp. Table S2, Supp. Table S3).

-Radiolabeled substrate uptake assays in X. laevis oocytes

Ecocyte Bio Science LLC (Austin, TX) provided stage VI, defollicuted oocytes along with oocyte injection services. Six to ten oocytes were selected per construct and each oocyte was injected with 50nL of saline, wild-type or mutant GLUT2 cRNA (40ng per oocyte). Oocytes were incubated on a shaker at 18°C in Modified Barth's solution with gentamicin (NaCl 88mM, KCl 1mM, $MgSO_4$ 1mM, HEPES 5mM, $NaHCO_3$ 2.5mM, $CaCl_2$ 0.7mM, Gentamicin 100μg/mL; Sigma-Aldrich) that was replenished every 24 hours. Forty-eight to seventy-two hours post-injection, thirty-minute uptake assays were performed using labeled [^{3}H]-2-deoxy-glucose (10μM total of 2-deoxy-glucose, PerkinElmer). Modified Barth's solution was used as the uptake buffer. Previous time range experiments revealed that 30 minutes was within the linear range of GLUT2 uptake (Supp. Figure S8). After uptake, oocytes were washed 5 times in cold uptake buffer then lysed in 0.5mL of 1% SDS (sodium dodecyl sulfate) solution (VWR International) for at least 1 hour. Radioactivity (disintegrations per minute) was measured using liquid scintillation counter machine. Radiolabeled substrate uptake rates were calculated by converting the DPM (disintegrations per minute) values of each oocyte to picomoles of substrate. Figures are representative of 3–5 experiments.

-Transfection and establishment of mammalian cell line transiently expressing GLUT2 reference and mutant cDNA.

Flp-In™ 293 cells (human embryonic kidney cells, Thermo Fisher Scientific) were transfected with select pcDNA5/FRT-GLUT2 mutant constructs using Lipofectamine® LTX with Plus™ reagent according to the manufacturer's instructions (Life Technologies) to confirm uptake and membrane expression results found in oocyte assays. Approximately 200,000 Flp-In™ 293 cells were plated in 24-well format; once each well reached 90% confluence, transient transfection was performed (4 replicates per construct). Transfected cells were maintained in DMEM containing 10% (v/v) FBS, 100 units/mL penicillin, 100 μg/mL streptomycin, and 100 μg/mL Zeocin (Thermo Fisher Scientific) at 37 °C and 5% CO_2 for 48 hours. Thereafter, thirty-minute uptake assays were performed using [^{3}H]-fructose (100 μM total of fructose). Cells were lysed for one hour using 800 μL of lysis buffer (0.1N NaOH, 0.1% SDS) and the radioactivity of 500μL of lysate was measured using a liquid scintillation counter machine. The DPM values were converted to picomoles of substrate. Total protein concentrations were determined using the bicinchoninic acid (BCA) assay using 25 μL of lysate per well (Thermo Fisher Scientific). Substrate uptake (in picomoles) was normalized by protein amount in each respective well.

-Plasma membrane expression assays

Forty-eight to seventy-two hours post oocyte injection, GLUT2 plasma membrane expression experiments were conducted for each FBS and population-specific mutant (6–10 oocytes). Oocytes were placed in blocking buffer (1% bovine serum albumin solution) for 30 minutes at 4°C. Next, oocytes were incubated in primary antibody solution (anti-GLUT2 mouse IgG antibody; MAB 1414, R&D systems) for 30 minutes at 4°C and then washed in blocking buffer six times. After washing, oocytes were transferred into secondary antibody solution (anti-mouse IgG VisUCyte HRP conjugate, R&D systems) for 30 minutes at 4°C then washed 6 times in blocking buffer and 6 times in ND96 buffer (NaCl 96mM, KCl 2mM, $CaCl_2$ 1.5mM, $MgCl_2$ 1mM, HEPES 5mM; Sigma-Aldrich). Each oocyte was transferred to the well of a white 96-well plate (catalog #3912, Corning Inc); 100 μL of SuperSignal ELISA Femto (Fisher Scientific) mix was added to each oocyte. One minute later, luminescence was measured using Glomax 96-well plate luminometer (Promega). All blocking and antibody solutions were produced using ND96 buffer. Plasma membrane expression was defined as a mutant transporter whose average luminescence's measurement was statistically similar to the average luminescence measurement of wild-type GLUT2. Figures are representative of 3–5 experiments.

-Kinetic studies of 2-deoxyglucose transport by GLUT2 and mutants

The transporter kinetics (V_{max} and K_m) of functional mutants were generated and compared with wild-type GLUT2. Uptake was linear between 0 – 40 minutes (0–60 minutes tested, Supp. Figure S8) so 30 minutes was selected to conduct uptake and kinetic studies. The thirty-minute uptake of [^{3}H]-2DG in a range of 2DG concentrations (0–100mM) was measured as previously described and plotted as rate of uptake versus concentration to generate non-linear regression curves. The K_m and V_{max} were calculated by fitting the curves to a Michaelis–Menten equation using GraphPad Prism 7 (La Jolla, CA).

-Statistical analysis

For comparison in radiolabeled uptake assays and plasma membrane expression assays, Student's t-test and one-way ANOVA statistical tests were performed. Statistical analyses, as specified in the legends of the figures and tables, were performed to determine significance, and a $p < 0.05$ was considered significant. Unless specified, data in figures and tables were expressed as mean ± standard error of the mean (SEM). All experiments were performed at least 3 to 5 times and in 6 to 10 oocytes or in 4 replicates in mammalian cell lines.

-Homology model construction for structural analysis

Homology models of GLUT2 were constructed with MODELLER v9.14 for mapping *SLC2A2* variants (Sali & Blundell, 1993). Specifically, three conformational states of GLUT2 were modeled: an inward-open state based on the human GLUT1 (PDB identifier 4PYP; sequence identity of 51.7%) (Deng et al., 2014); an occluded state based on a *Escherichia coli* XylE transporter structure (4GC0; 23.8%) (Sun et al., 2012); and an outward-open state based on the human GLUT3 (4ZWC; 48.1%) (Deng et al., 2015). The alignment between GLUT2 and the template was generated using Promals3D (Pei & Grishin, 2014). The models were evaluated and ranked with Z-DOPE (Shen & Sali, 2006) obtaining scores of −0.70, −1.20, and −0.85, suggesting they are sufficiently accurate for further analysis.

To deduce the structural effects of the FBS missense variants on *SLC2A2*, variants that were functionally evaluated and expressed on the plasma membrane (nine mutations) were modeled and studied using molecular dynamics (MD) simulations. CHARMM-GUI Membrane Builder (Wu et al., 2014) was used to construct and introduce the variants to the GLUT2 homology model in the outward-open conformation in lipid bilayer for MD simulations (Lee et al., 2016). Protein and the lipid bilayer system were parameterized with AMBER formatted CHARMM36m force fields (Brooks et al., 2009; Huang et al., 2017). Cholesterol (10%), phosphatidylcholine DOPC (55%), and phosphatidylethanolamine DOPE (35%) were used to construct the system in rectangular box with same x and y dimensions and at least 18 Å from protein to box edge. The final average area of the lipid bilayer was 7,600 $Å^2$ with 13,704 TIP3P water molecules (Jorgensen et al., 1983) and 0.15M NaCl concentration, with ~ 72,500–72,600 atoms for the various mutations. AMBER16 GPU-enabled PMEMD was used to perform the MD simulations (Case et al., 2018; Salomon-Ferrer et al., 2013). The systems were minimized with 500 steps and equilibrated with NVT and NPT at 310.15 K, while hydrogens were constrained with SHAKE to enable 2-fs time step (Ryckaert, Ciccotti, & Berendsen, 1977). 1 ns of equilibration followed by 25 ns production run were performed for all systems. Trajectories were analyzed with CPPTRAJ (Roe & Cheatham, 2013) and visualized with PyMOL (The PyMOL Molecular Graphics System, Version 1.7 Schrödinger, LLC).

Supplementary Material

Refer to Web version on PubMed Central for supplementary material.

Acknowledgements

We thank Dr. Graeme I Bell (University of Chicago) for the generous gift of pSP64T-GLUT2 plasmid, Dr. David L Minor Jr for allowing the generous use of his oocyte incubator and members of the Minor lab (Lianne Pope, Fayal Abderemaneali) for their guidance in performing oocyte injection and membrane expression assays. We also like to acknowledge Dr. Renata Gallagher for her helpful discussions.

Funding

This work was supported by the National Institutes of Health [GM117163 to K.M.G. and S.W.Y, GM108911 to K.M.G., R25 GM56847 to A.S.], the Burroughs Wellcome Fund [BWF ID 1012485 to K.M.G.] and a grant to the University of California San Francisco from the Howard Hughes Medical Institute through the James H. Gilliam Fellowships for Advanced Study Program (to O.J.E.).

REFERENCES:

Abbasi F, Azizi F, Javaheri M, Mosallanejad A, Ebrahim-Habibi A, & Ghafouri-Fard S (2015). Segregation of a novel homozygous 6 nucleotide deletion in GLUT2 gene in a Fanconi-Bickel syndrome family. Gene, 557(1), 103–105. 10.1016/j.gene.2014.12.024 [PubMed: 25523092]

Adzhubei IA, Schmidt S, Peshkin L, Ramensky VE, Gerasimova A, Bork P, … Sunyaev SR (2010). A method and server for predicting damaging missense mutations. Nature Methods, 7(4), 248–249. 10.1038/nmeth0410-248 [PubMed: 20354512]

Amita M, Srivastava P, & Mandal K (2017). Fanconi-Bickel Syndrome : Another Novel Mutation in SLC2A2, 84(March), 236–237. 10.1007/s12098-016-2236-6

Asjad HMM, Kasture A, El-Kasaby A, Sackel M, Hummel T, Freissmuth M, & Sucic S (2017). Pharmacochaperoning in a Drosophila model system rescues human dopamine transporter variants associated with infantile/juvenile parkinsonism. The Journal of Biological Chemistry, 292(47), 19250–19265. 10.1074/jbc.M117.797092 [PubMed: 28972153]

Bahíllo-Curieses MP, Garrote-Molpeceres R, Miñambres-Rodríguez M, del Real-Llorente MR, Tobar-Mideros C, & Rellán-Rodríguez S (2017). Glycosuria and hyperglycemia in the neonatal period as the first clinical sign of Fanconi-Bickel syndrome. Pediatric Diabetes. 10.1111/pedi.12531

Barker A, Sharp SJ, Timpson NJ, Bouatia-Naji N, Warrington NM, Kanoni S, … Langenberg C (2011). Association of genetic Loci with glucose levels in childhood and adolescence: a meta-analysis of over 6,000 children. Diabetes, 60(6), 1805–1812. 10.2337/db10-1575 [PubMed: 21515849]

Baron D, Assaraf YG, Cohen N, & Aronheim A (2002). Lack of plasma membrane targeting of a G172D mutant thiamine transporter derived from Rogers syndrome family. Molecular Medicine (Cambridge, Mass.), 8(8), 462–74. http://doi.org/S1528365802804621 [pii]

Baroudi G, Carbonneau E, Pouliot V, & Chahine M (2000). SCN5A mutation (T1620M) causing Brugada syndrome exhibits different phenotypes when expressed in Xenopus oocytes and mammalian cells. FEBS Letters, 467(1), 12–16. [PubMed: 10664447]

Baroudi G, Pouliot V, Denjoy I, Guicheney P, Shrier A, & Chahine M (2001). Novel mechanism for Brugada syndrome: defective surface localization of an SCN5A mutant (R1432G). Circulation Research, 88(12), E78–83. [PubMed: 11420310]

Berry GT, Baker L, Kaplan FS, & Witzleben CL (1995). Diabetes-like renal glomerular disease in Fanconi-Bickel syndrome. Pediatric Nephrology, 9(3), 287–291. 10.1007/BF02254185 [PubMed: 7632512]

Blot V, & McGraw TE (2008). Molecular mechanisms controlling GLUT4 intracellular retention. Molecular Biology of the Cell, 19(8), 3477–3487. 10.1091/mbc.e08-03-0236 [PubMed: 18550797]

Brooks BR, Brooks CL, Mackerell AD, Nilsson L, Petrella RJ, Roux B, … Karplus M (2009). CHARMM: The biomolecular simulation program. Journal of Computational Chemistry, 30(10), 1545–1614. 10.1002/jcc.21287 [PubMed: 19444816]

Case DA, Ben-Shalom IY, Brozell SR, Cerutti DS,. Cheatham TE III, Cruzeiro VWD, Darden TA, Duke RE, Ghoreishi D, Gilson MK, Gohlke H, Goetz AW, Greene D, Harris R, Homeyer N, Izadi S, Kovalenko A, Kurtzman T, Lee TS, LeGra S, D. M. Y. and P. A. K. (2018). AMBER18. University of California, San Francisco.

Colas C, Ung PM-U, & Schlessinger A (2016). SLC Transporters: Structure, Function, and Drug Discovery. MedChemComm, 7(6), 1069–1081. 10.1039/C6MD00005C [PubMed: 27672436]

Consortium T. 1000 G. P. (2015). A global reference for human genetic variation. Nature, 526(7571), 68–74. 10.1038/nature15393 [PubMed: 26432245]

Cooper GM, Stone EA, Asimenos G, Green ED, Batzoglou S, & Sidow A (2005). Distribution and intensity of constraint in mammalian genomic sequence. Genome Research, 15(7), 901–913. 10.1101/gr.3577405 [PubMed: 15965027]

Deng D, Sun P, Yan C, Ke M, Jiang X, Xiong L, … Yan N (2015). Molecular basis of ligand recognition and transport by glucose transporters. Nature, 526(7573), 391–396. 10.1038/nature14655 [PubMed: 26176916]

Deng D, Xu C, Sun P, Wu J, Yan C, Hu M, & Yan N (2014). Crystal structure of the human glucose transporter GLUT1. Nature, 510(7503), 121–125. 10.1038/nature13306 [PubMed: 24847886]

Denning GM, Anderson MP, Amara JF, Marshall J, Smith AE, & Welsh MJ (1992). Processing of mutant cystic fibrosis transmembrane conductance regulator is temperature-sensitive. Nature, 358(6389), 761–764. 10.1038/358761a0 [PubMed: 1380673]

Dupuis J, Langenberg C, Prokopenko I, Saxena R, Soranzo N, Jackson AU, … Barroso I (2010). New genetic loci implicated in fasting glucose homeostasis and their impact on type 2 diabetes risk. Nature Genetics, 42(2), 105–116. 10.1038/ng.520 [PubMed: 20081858]

El-Kasaby A, Koban F, Sitte HH, Freissmuth M, & Sucic S (2014). A cytosolic relay of heat shock proteins HSP70–1A and HSP90beta monitors the folding trajectory of the serotonin transporter. The Journal of Biological Chemistry, 289(42), 28987–29000. 10.1074/jbc.M114.595090 [PubMed: 25202009]

Fanconi G, & Bickel H (1949). Chronic aminoaciduria (amino acid diabetes or nephrotic-glucosuric dwarfism) in glycogen storage and cystine disease. Helvetica paediatrica acta, 4(5), 359–396. [PubMed: 15397919]

Geno2MP, NHGRI/NHLBI University of Washington-Center for Mendelian Genomics (UW-CMG), Seattle, WA (n.d.). Retrieved from http://geno2mp.gs.washington.edu

Grünert SC, Schwab KO, Pohl M, Sass JO, & Santer R (2012). Fanconi-Bickel syndrome: GLUT2 mutations associated with a mild phenotype. Molecular Genetics and Metabolism, 105(3), 433–437. 10.1016/j.ymgme.2011.11.200 [PubMed: 22214819]

Gupta N, Nambam B, Weinstein DA, & Shoemaker LR (2016). Late Diagnosis of Fanconi-Bickel Syndrome. Journal of Inborn Errors of Metabolism and Screening, 4, 232640981667943 10.1177/2326409816679430

Hadipour F, Sarkheil P, Noruzinia M, Hadipour Z, Baghdadi T, & Shafeghati Y (2013). Fanconi-Bickel syndrome versus osteogenesis imperfeeta: An Iranian case with a novel mutation in glucose transporter 2 gene, and review of literature. Indian Journal of Human Genetics, 19(1), 84–86. 10.4103/0971-6866.112906 [PubMed: 23901198]

Huang J, Rauscher S, Nawrocki G, Ran T, Feig M, de Groot BL, … MacKerell ADJ (2017). CHARMM36m: an improved force field for folded and intrinsically disordered proteins. Nature Methods, 14(1), 71–73. 10.1038/nmeth.4067 [PubMed: 27819658]

Inukai K, Shewan AM, Pascoe WS, Katayama S, James DE, & Oka Y (2004). Carboxy terminus of glucose transporter 3 contains an apical membrane targeting domain. Molecular Endocrinology (Baltimore, Md.), 18(2), 339–349. 10.1210/me.2003-0089

Ioannidis NM, Rothstein JH, Pejaver V, Middha S, McDonnell SK, Baheti S, … Sieh W (2016). REVEL: An Ensemble Method for Predicting the Pathogenicity of Rare Missense Variants. American Journal of Human Genetics, 99(4), 877–885. 10.1016/j.ajhg.2016.08.016 [PubMed: 27666373]

Jorgensen WL, Chandrasekhar J, Madura JD, Impey RW, & Klein ML (1983). Comparison of simple potential functions for simulating liquid water. The Journal of Chemical Physics, 79(2), 926–935. 10.1063/1.445869

Karamizadeh Z, Saki F, Imanieh MH, Zahmatkeshan M, & Fardaee M (2012). A new mutation of Fanconi-Bickel syndrome with liver failure and pseudotumour cerebri. Journal of Genetics, 91(3), 359–361. 10.1007/s12041-012-0198-7 [PubMed: 23271022]

Karniski LP (2001). Mutations in the diastrophic dysplasia sulfate transporter (DTDST) gene: correlation between sulfate transport activity and chondrodysplasia phenotype. Human Molecular Genetics, 10(14), 1485–1490. [PubMed: 11448940]

Karniski LP (2004). Functional expression and cellular distribution of diastrophic dysplasia sulfate transporter (DTDST) gene mutations in HEK cells. Human Molecular Genetics, 13(19), 2165–2171. 10.1093/hmg/ddh242 [PubMed: 15294877]

Kircher M, Witten DM, Jain P, O'Roak BJ, Cooper GM, & Shendure J (2014). A general framework for estimating the relative pathogenicity of human genetic variants. Nature Genetics, 46(3), 310–315. 10.1038/ng.2892 [PubMed: 24487276]

Koban F, El-Kasaby A, Hausler C, Stockner T, Simbrunner BM, Sitte HH, … Sucic S (2015). A salt bridge linking the first intracellular loop with the C terminus facilitates the folding of the serotonin transporter. The Journal of Biological Chemistry, 290(21), 13263–13278. 10.1074/jbc.M115.641357 [PubMed: 25869136]

Kundu K, & Backofen R (2014). Cluster based prediction of PDZ-peptide interactions. BMC Genomics, 15 Suppl 1, S5 10.1186/14712164-15-S1-S5

Kundu K, Costa F, Huber M, Reth M, & Backofen R (2013). Semisupervised prediction of SH2-peptide interactions from imbalanced highthroughput data. PloS One, 8(5), e62732 10.1371/journal.pone.0062732 [PubMed: 23690949]

Kundu K, Mann M, Costa F, & Backofen R (2014). MoDPepInt: an interactive web server for prediction of modular domain-peptide interactions. Bioinformatics (Oxford, England), 30(18), 2668–2669. 10.1093/bioinformatics/btu350

Lee EE, Ma J, Sacharidou A, Mi W, Salato VK, Nguyen N, … Wang RC (2015). A Protein Kinase C Phosphorylation Motif in GLUT1 Affects Glucose Transport and is Mutated in GLUT1 Deficiency Syndrome. Molecular Cell, 58(5), 845–853. 10.1016/j.molcel.2015.04.015 [PubMed: 25982116]

Lee J, Cheng X, Swails JM, Yeom MS, Eastman PK, Lemkul JA, … Im W (2016). CHARMM-GUI Input Generator for NAMD, GROMACS, AMBER, OpenMM, and CHARMM/OpenMM Simulations Using the CHARMM36 Additive Force Field. Journal of Chemical Theory and Computation, 12(1), 405–413. 10.1021/acs.jctc.5b00935 [PubMed: 26631602]

Lek M, Karczewski KJ, Minikel EV, Samocha KE, Banks E, Fennell T, … MacArthur DG (2016). Analysis of protein-coding genetic variation in 60,706 humans. Nature, 536(7616), 285–291. 10.1038/nature19057 [PubMed: 27535533]

Machamer CE, & Rose JK (1988). Vesicular stomatitis virus G proteins with altered glycosylation sites display temperature-sensitive intracellular transport and are subject to aberrant intermolecular disulfide bonding. Journal of Biological Chemistry, 263(12), 5955–5960. [PubMed: 2833524]

Machiela MJ, & Chanock SJ (2018). LDassoc: an online tool for interactively exploring genome-wide association study results and prioritizing variants for functional investigation. Bioinformatics (Oxford, England), 34(5), 887–889. 10.1093/bioinformatics/btx561

Manning AK, Hivert M-F, Scott RA, Grimsby JL, Bouatia-Naji N, Chen H, … Langenberg C (2012). A genome-wide approach accounting for body mass index identifies genetic variants influencing fasting glycemic traits and insulin resistance. Nature Genetics, 44(6), 659–669. 10.1038/ng.2274 [PubMed: 22581228]

Mannstadt M, Magen D, Segawa H, Stanley T, Sharma A, Sasaki S, … Jüppner H (2012). Fanconi-Bickel syndrome and autosomal recessive proximal tubulopathy with hypercalciuria (ARPTH) are allelic variants caused by GLUT2 mutations. Journal of Clinical Endocrinology and Metabolism, 97(10), 1978–1986. 10.1210/jc.2012-1279

Manz F, Bickel H, Brodehl J, Feist D, Gellissen K, Gescholl-Bauer B, … Waldherr R (1987). Pediatric Nephrology. Pediatric Nephrology, 1(October 1960), 509–518. [PubMed: 3153325]

Michau A, Guillemain G, Grosfeld A, Vuillaumier-Barrot S, Grand T, Keck M, … Le Gall M (2013). Mutations in SLC2A2 Gene Reveal hGLUT2 Function in Pancreatic β Cell Development. The Journal of Biological Chemistry, 288(43), 31080–31092. 10.1074/jbc.M113.469189 [PubMed: 23986439]

Mueckler M, & Thorens B (2013). The SLC2 (GLUT) family of membrane transporters. Molecular Aspects of Medicine, 34(2–3), 121–138. 10.1016/j.mam.2012.07.001 [PubMed: 23506862]

Ng PC, & Henikoff S (2003). SIFT: predicting amino acid changes that affect protein function. Nucleic Acids Research, 31(13), 3812–3814. Retrieved from 10.1093/nar/gkg509 [PubMed: 12824425]

Odièvre MH, Lombès A, Dessemme P, Santer R, Brivet M, Chevallier B, … Odièvre M (2002). A secondary respiratory chain defect in a patient with Fanconi-Bickel syndrome. Journal of Inherited Metabolic Disease, 25(5), 379–384. 10.1023/A:1020147716990 [PubMed: 12408187]

Peduto A, Spada M, Alluto A, La Dolcetta M, Ponzone A, & Santer R (2004). A novel mutation in the GLUT2 gene in a patient with Fanconi-Bickel syndrome detected by neonatal screening for galactosaemia. Journal of Inherited Metabolic Disease, 27(2), 279–280. [PubMed: 15243984]

Pei J, & Grishin NV (2014). PROMALS3D: multiple protein sequence alignment enhanced with evolutionary and three-dimensional structural information. Methods in Molecular Biology (Clifton, N.J.), 1079, 263–271. 10.1007/978-1-62703-646-7_17

Pogoriler J, Neill AFO, Voss SD, Shamberger RC, & Perez-atayde AR (2017). Hepatocellular Carcinoma in Fanconi-Bickel Syndrome. 10.1177/1093526617693540

Pollard KS, Hubisz MJ, Rosenbloom KR, & Siepel A (2010). Detection of nonneutral substitution rates on mammalian phylogenies. Genome Research, 20(1), 110–121. 10.1101/gr.097857.109 [PubMed: 19858363]

Raja M, & Kinne RKH (2015). Pathogenic mutations causing glucose transport defects in GLUT1 transporter: The role of intermolecular forces in protein structure-function. Biophysical Chemistry, 200–201, 9–17. 10.1016/j.bpc.2015.03.005

Roe DR, & Cheatham TE 3rd. (2013). PTRAJ and CPPTRAJ: Software for Processing and Analysis of Molecular Dynamics Trajectory Data. Journal of Chemical Theory and Computation, 9(7), 3084–3095. 10.1021/ct400341p [PubMed: 26583988]

Ryckaert J-P, Ciccotti G, & Berendsen HJC (1977). Numerical integration of the cartesian equations of motion of a system with constraints: molecular dynamics of n-alkanes. Journal of Computational Physics, 23(3), 327–341.

Sakamoto O, Ogawa E, Ohura T, Igarashi Y, Matsubara Y, Narisawa K, & Iinuma K (2000). Mutation analysis of the GLUT2 gene in patients with Fanconi-Bickel syndrome. Pediatric Research, 48(5), 586–9. 10.1203/00006450-200011000-00005 [PubMed: 11044475]

Sali A, & Blundell TL (1993). Comparative protein modelling by satisfaction of spatial restraints. Journal of Molecular Biology, 234(3), 779–815. 10.1006/jmbi.1993.1626 [PubMed: 8254673]

Salomon-Ferrer R, Götz AW, Poole D, Le Grand S, & Walker RC (2013). Routine Microsecond Molecular Dynamics Simulations with AMBER on GPUs. 2. Explicit Solvent Particle Mesh Ewald. Journal of Chemical Theory and Computation, 9(9), 3878–3888. 10.1021/ct400314y [PubMed: 26592383]

Santer R, Groth S, Kinner M, Dombrowski A, Berry GT, Brodehl J, … Schaub J (2002). The mutation spectrum of the facilitative glucose transporter gene SLC2A2 (GLUT2) in patients with Fanconi-Bickel syndrome. Human Genetics, 110(1), 21–29. 10.1007/s00439001-0638-6 [PubMed: 11810292]

Santer R, Schneppenheim R, Dombrowski A, Gotze H, Steinmann B, & Schaub J (1997). Mutations in GLUT2, the gene for the liver-type glucose transporter, in patients with Fanconi-Bickel syndrome. Nature Genetics, 17(3), 324–326. 10.1038/ng1197-324 [PubMed: 9354798]

Santer R, Schneppenheim R, Suter D, Schaub J, & Steinmann B (1998). Fanconi-Bickel syndrome - The original patient and his natural history, historical steps leading to the primary defect, and a review of the literature. European Journal of Pediatrics, 157(10), 783–797. 10.1007/s004310050937 [PubMed: 9809815]

Scott RA, Scott LJ, Magi R, Marullo L, Gaulton KJ, Kaakinen M, … Prokopenko I (2017). An Expanded Genome-Wide Association Study of Type 2 Diabetes in Europeans. Diabetes, 66(11), 2888–2902. 10.2337/db16-1253 [PubMed: 28566273]

Seatter MJ, De la Rue SA, Porter LM, & Gould GW (1998). QLS motif in transmembrane helix VII of the glucose transporter family interacts with the C-1 position of D-glucose and is involved in substrate selection at the exofacial binding site. Biochemistry, 37(5), 1322–1326. 10.1021/bi972322u [PubMed: 9477959]

Shen M-Y, & Sali A (2006). Statistical potential for assessment and prediction of protein structures. Protein Science : A Publication of the Protein Society, 15(11), 2507–2524. 10.1110/ps.062416606 [PubMed: 17075131]

Sigel E (1990). Use of Xenopus oocytes for the functional expression of plasma membrane proteins. J Membr Biol, 117(3), 201–221. 10.1007/BF01868451 [PubMed: 2231695]

Skach WR (2000). Defects in processing and trafficking of the cystic fibrosis transmembrane conductance regulator. Kidney International, 57(3), 825–831. 10.1046/j.1523-1755.2000.00921.x [PubMed: 10720935]

Su Z, Du ML, Chen HS, Chen QL, Yu CS, & Ma HM (2011). Two cases of Fanconi-Bickel syndrome: First report from China with novel mutations of SLC2A2 gene. Journal of Pediatric Endocrinology and Metabolism, 24(9–10), 749–753. 10.1515/JPEM.2011.316 [PubMed: 22145468]

Sun L, Zeng X, Yan C, Sun X, Gong X, Rao Y, & Yan N (2012). Crystal structure of a bacterial homologue of glucose transporters GLUT1–4. Nature, 490(7420), 361–366. 10.1038/nature11524 [PubMed: 23075985]

Toye AM (2005). Defective kidney anion-exchanger 1 (AE1, Band 3) trafficking in dominant distal renal tubular acidosis (dRTA). Biochemical Society Symposium, (72), 47–63. [PubMed: 15649129]

Type 2 Diabetes Knowledge Portal. (n.d.). Retrieved March 15, 2017, from http://www.type2diabetesgenetics.org/variantInfo/variantInfo/rs140138702#

Ung PM-U, Song W, Cheng L, Zhao X, Hu H, Chen L, & Schlessinger A (2016). Inhibitor Discovery for the Human GLUT1 from Homology Modeling and Virtual Screening. ACS Chemical Biology, 11(7), 1908–1916. 10.1021/acschembio.6b00304 [PubMed: 27128978]

von Heijne G (1991). Proline kinks in transmembrane alpha-helices. Journal of Molecular Biology, 218(3), 499–503. [PubMed: 2016741]

Wang W, Wei M, Song HM, Qiu ZQ, Zhang LJ, Li Z, & Tang XY (2015). SLC2A2 gene analysis in three Chinese children with Fanconi-Bickel syndrome. Chinese Journal of Contemporary Pediatrics, 17(4), 362–366. 10.7499/j.issn.1008-8830.2015.04.014 [PubMed: 25919556]

Waterhouse AM, Procter JB, Martin DMA, Clamp M, & Barton GJ (2009). Jalview Version 2—a multiple sequence alignment editor and analysis workbench. Bioinformatics, 25(9), 1189–1191. Retrieved from 10.1093/bioinformatics/btp033 [PubMed: 19151095]

Wheeler E, Leong A, Liu C-T, Hivert M-F, Strawbridge RJ, Podmore C, … Meigs JB (2017). Impact of common genetic determinants of Hemoglobin A1c on type 2 diabetes risk and diagnosis in ancestrally diverse populations: A transethnic genome-wide meta-analysis. PLoS Medicine, 14(9), e1002383 10.1371/journal.pmed.1002383 [PubMed: 28898252]

Wieman HL, Horn SR, Jacobs SR, Altman BJ, Kornbluth S, & Rathmell JC (2009). An essential role for the Glut1 PDZ-binding motif in growth factor regulation of Glut1 degradation and trafficking. Biochemical Journal, 418(2), 345–367. 10.1042/BJ20081422 [PubMed: 19016655]

Woodward OM, Tukaye DN, Cui J, Greenwell P, Constantoulakis LM, Parker BS, … Guggino WB (2013). Gout-causing Q141K mutation in ABCG2 leads to instability of the nucleotide-binding domain and can be corrected with small molecules. Proceedings of the National Academy of Sciences, 110(13), 5223–5228. 10.1073/pnas.1214530110

Wu EL, Cheng X, Jo S, Rui H, Song KC, Davila-Contreras EM, … Im W (2014). CHARMM-GUI Membrane Builder toward realistic biological membrane simulations. Journal of Computational Chemistry, 35(27), 1997–2004. 10.1002/jcc.23702 [PubMed: 25130509]

Yoo HW, Shin YL, Seo EJ, & Kim GH (2002). Identification of a novel mutation in the GLUT2 gene in a patient with Fanconi-Bickel syndrome presenting with neonatal diabetes mellitus and galactosaemia. European Journal of Pediatrics, 161(6), 351–353. 10.1007/s00431-0020931-y [PubMed: 12029458]

Zhou K, Yee SW, MetGen coauthors, Giacomini K, P. E. (2016). Variation in the Glucose transporter gene GLUT2 (SLC2A2) is associated with glycaeic response to metformin: A MetGen study.

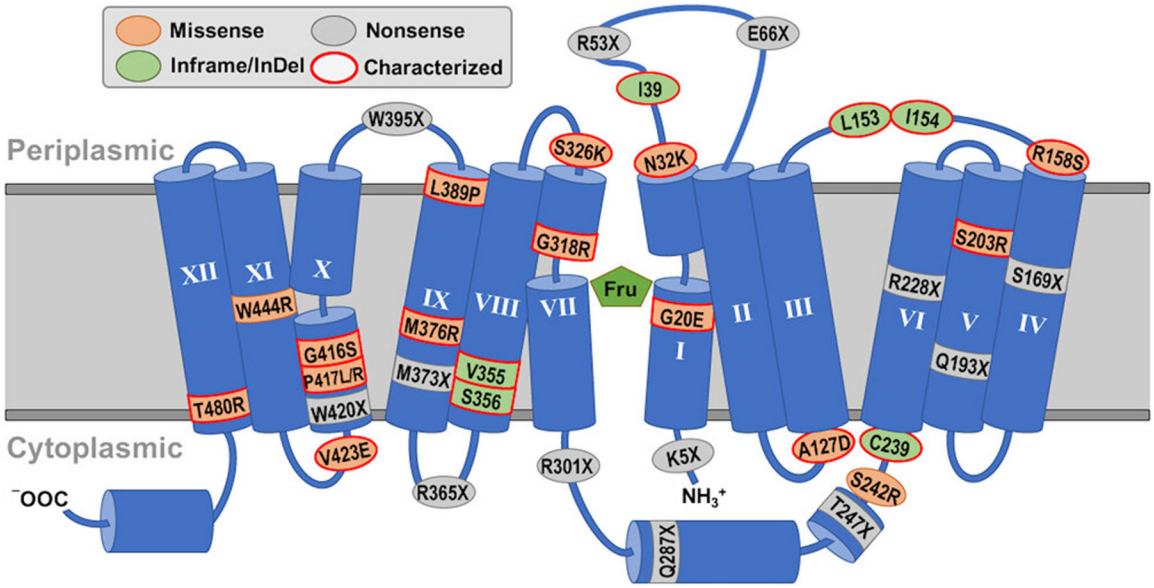

Figure 1:

Fanconi-Bickel syndrome (FBS) variant location within GLUT2 transporter structure. An illustration of the GLUT2 that displays the location of all published missense (orange), nonsense (grey), and in-frame indel (green) *SLC2A2* variants associated with FBS. The majority of these FBS variants had not been evaluated in-vitro to test their impact on GLUT2 membrane expression or function. We selected seventeen variants (red border) to functionally characterize in our study. Roman numerals I-XII represent each transmembrane helix in the GLUT2. The green pentagon labeled “Fru” represents fructose.

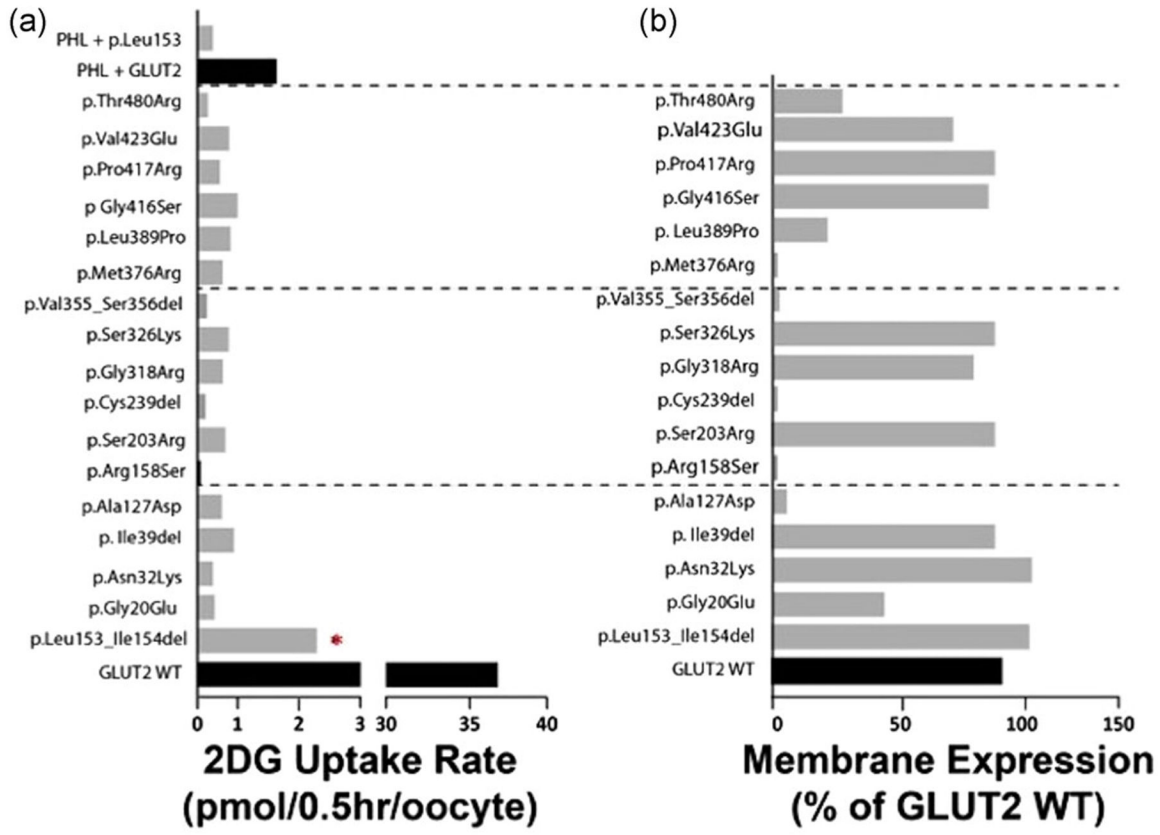

Figure 2.

FBS mutant transporter uptake and plasma membrane expression. The first graph shows average transport rate of cRNA-injected *X. laevis* oocytes incubated with uptake buffer containing [^{3}H]-2DG and 10μM of unlabeled 2DG for 30 minutes. All FBS mutant transporters had significantly reduced uptake of substrate compared with wild-type GLUT2 (one-way ANOVA F = 467.7; p-value < 0.0001) except for p.Leu153_Ile154del, which had significantly higher 2DG uptake compared to the other FBS mutants (one-way ANOVA F = 5.591, *p-value = 0.0006). The second graph shows luminescence emitted by cRNA-injected oocytes incubated sequentially with anti-GLUT2 (MAB #1414, R&D systems) and HRP-conjugated antibodies. Nine of the seventeen evaluated FBS mutant transporters were expressed on the plasma membrane at similar levels to wild-type GLUT2 (one-way ANOVA F-value = 0.6534; p-value = 0.74). The other eight mutants had partial or negligible plasma membrane expression compared with wild-type (one-way ANOVA F-value = 23.05; p-value < 0.0001). “PHL” in the figure represents phloretin, a canonical inhibitor of GLUT transporters. Data shown represent the mean ± SEM for 3 – 5 independent experiments.

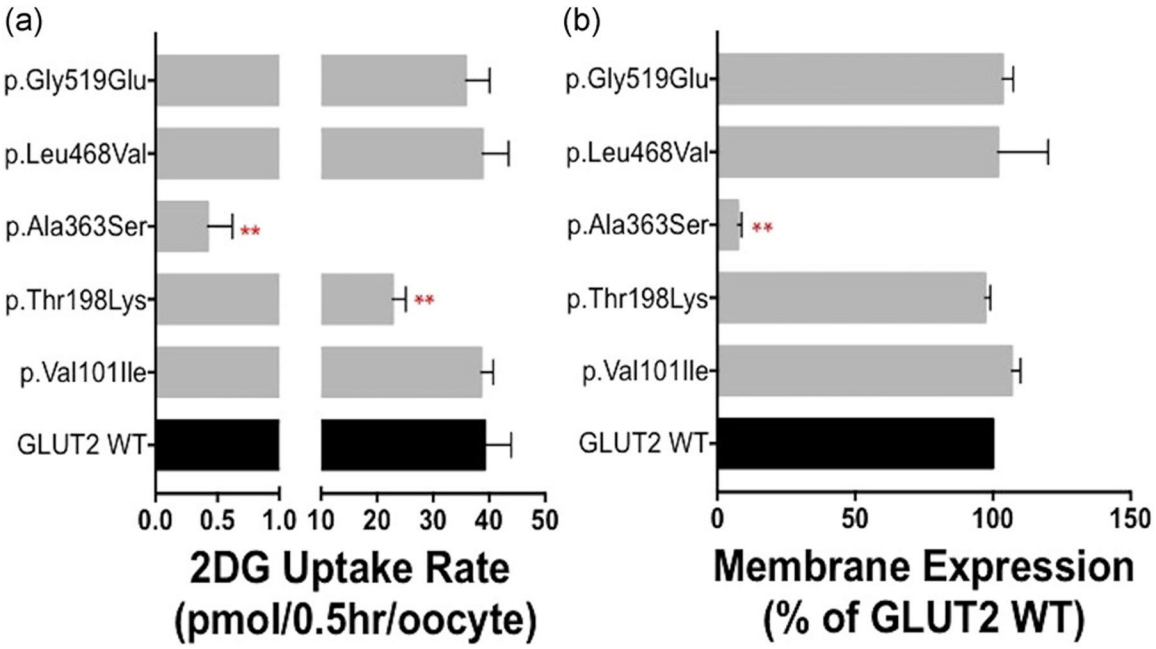

Figure 3.

Less common mutant transporter uptake and plasma membrane expression. Figure 3a shows average transport rate of cRNA-injected *X. laevis* oocytes incubated with uptake buffer containing [^{3}H]-2DG and 10μM of unlabeled 2DG for 30 minutes. The uptake rate of three out of the five mutant transporters (p.Val101Ile, p. Leu468Vale, p.Gly519Glu) was comparable to that of wild-type GLUT2 (one way ANOVA F= 0.1149; p-value =0.9509). The uptake rate of p.Thr198Lys (12 pmol/0.5hr/oocyte) was 42% lower than that of wild-type GLUT2 (40 pmol/0.5hr/oocyte, student t-test **p-value ≤ 0.0056). The uptake rate of p.Ala363Ser was negligible and similar to saline-injected oocytes. Figure 3b shows luminescence emitted by cRNA-injected oocytes incubated with anti-GLUT2 then HRP-conjugated antibodies. All mutant transporters were expressed on the plasma membrane in similar levels to that of wild-type GLUT2 (one way ANOVA F value = 0.3502, p-value = 0.88) except for p.Ala363Ser, which was not expressed on the oocyte plasma membrane (students t-test 7.4% vs 100%, **p-value < 0.0001). Data shown represent the mean ± SEM for 3 – 5 independent experiments.

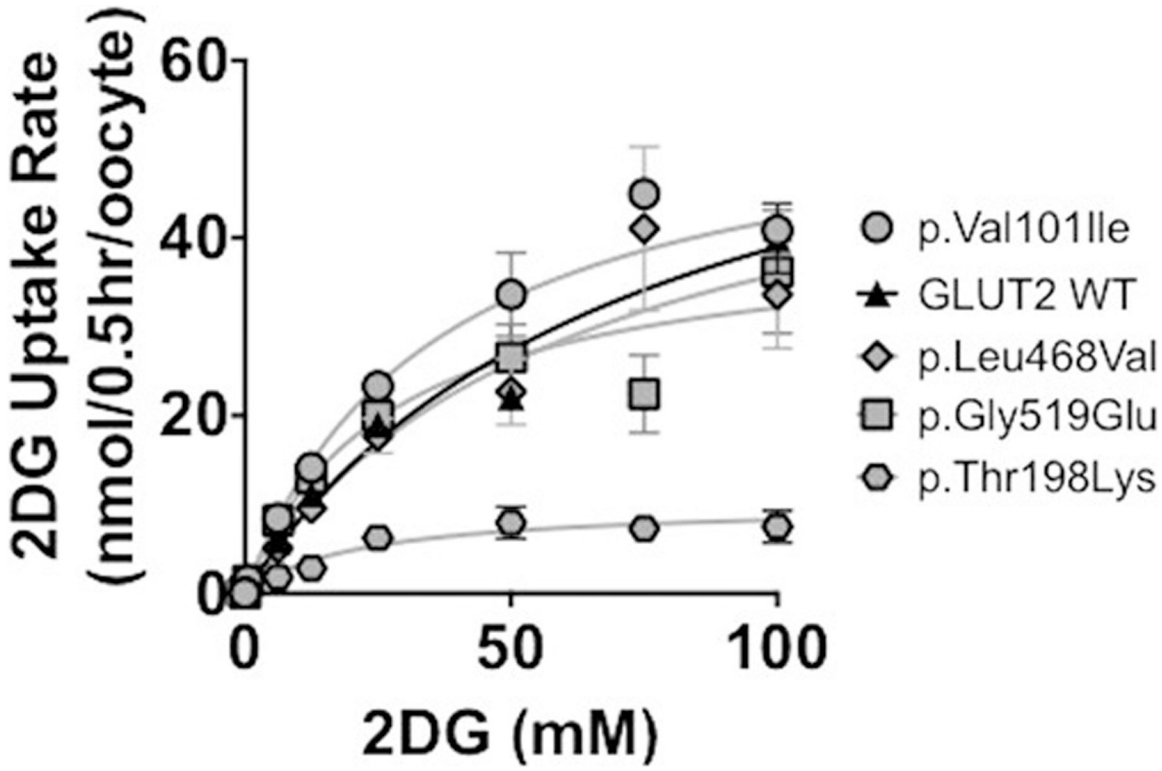

Figure 4.

Kinetic characterization of less common variants using [^{3}H]-2DG. Michaelis-Menten curves for each population-specific variant were generated using 2DG concentrations ranging from 0.001 to 100mM. K_m and V_{max} values of each mutant with the exception of p.Ala363Ser were calculated by fitting the data to a non-linear regression curve. The K_m and V_{max} values of each mutant (mean + SEM) are listed in Table 1.

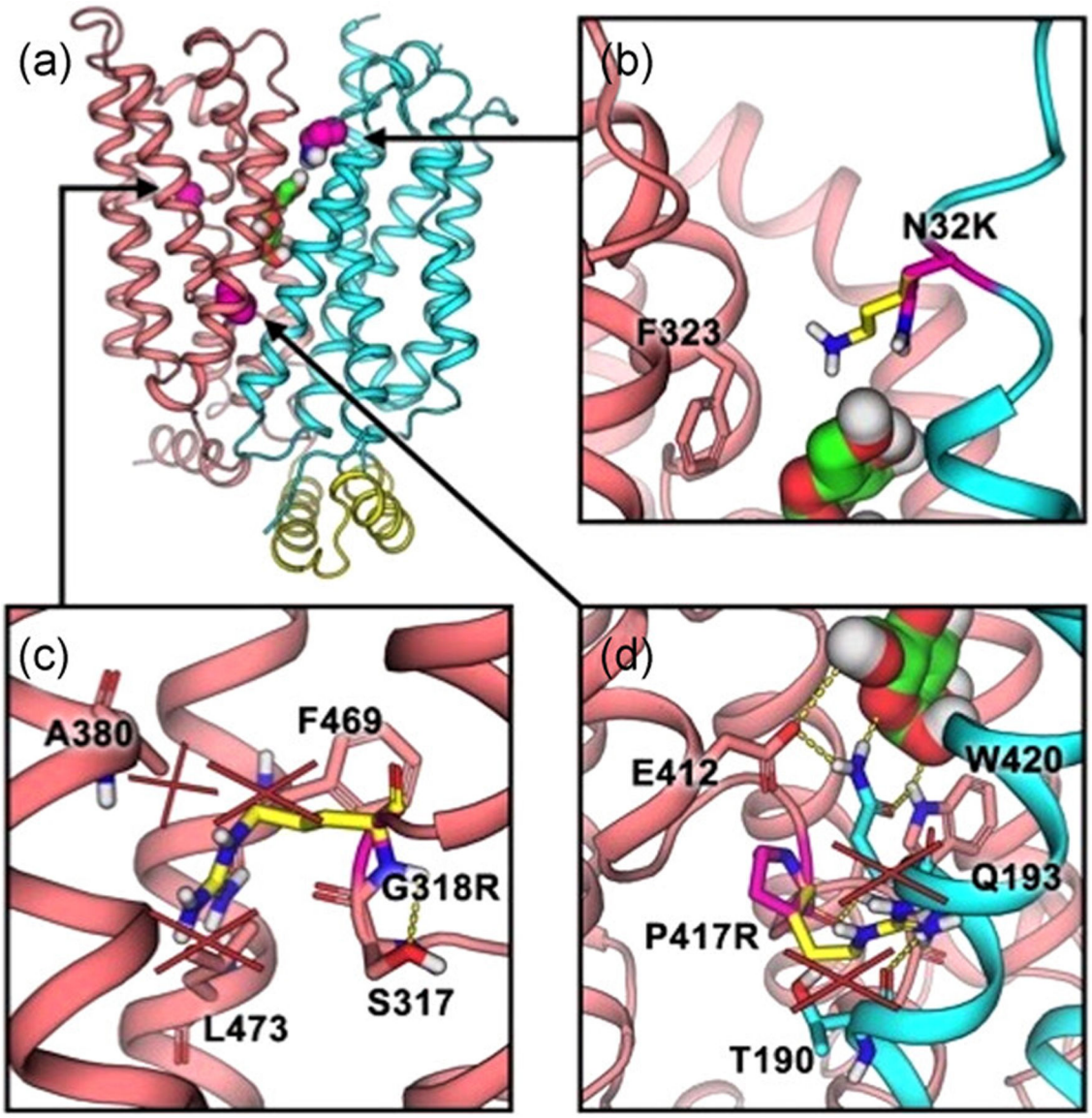

Figure 5.

Structural analysis of GLUT2 variants associated with FBS. (a) GLUT2 homology model in an outward-open conformation. TM1–6, intracellular helix, and TM7–12 are represented as cyan, yellow, and salmon cartoon, respectively; the sugar maltose, derived from the template structure, is depicted as green sticks. Residues of interest and their mutations are depicted as magenta and yellow sticks, respectively. (b) Asn32 locates on TM2 and exposes to the extracellular channel. p.Asn32Lys (N32K) extends the reach of the residue sidechain into the channel by ~ 3.0 Å, potentially hindering the entry of substrate. (c) Gly318 on TM7 is flanked by several bulky residues on TM9 and TM12, in addition to forms part of the SGXXG helix kink on TM7. p.Gly318Arg (G318R) mutation introduces a bulky sidechain that clashes with bulky sidechains of TM9 and TM12 that disrupts the helix-helix packing interface, while affecting the formation of the native kink on TM7. (d) Pro417 forms part of the TM10 helix kink and packs against TM5 and TM8, where its backbone carbonyl

participates in the hydrogen-bond network of the substrate-binding site through interaction with the conserved Gln314 and Trp420. p.Pro417Arg (P417R) mutation, and similarly p.Pro417Leu, alters the formation of th TM10 helix kink. Furthermore, the introduction of a bulky sidechain clashes with Thr190 and Gln193, which disrupts the packing of TM5, TM8, TM10 as well as the integrity of the hydrogen-bond network of the substrate-binding site. Hydrogen bonds and steric clashes are depicted as yellow dotted lines and red crosses, respectively.

Table 1.

Estimated kinetic parameters (K_m, V_{max}) for 2DG transport by GLUT2 less common variants. The K_m values for the four measured mutants are statistically similar to wild-type GLUT2 (one-way ANOVA p-value = 0.44). The V_{max} values of these mutants are also similar (one-way ANOVA p-value = 0.48) except for the significantly reduced V_{max} of p.Thr198Leu when compared with wild-type GLUT2 (11.7 vs 52.7, students t-test ***p-value = 0.0044). K_m and V_{max} shown represent the mean and standard error [mean (SE)] for 2 independent experiments.

	K_m (mM) [mean (SE)]	**V_{max} (nmol/0.5hr/oocyte) [mean (SE)]**
GLUT2 WT	34 (3.3)	53 (2.0)
c.301G>A (p.Val101lle)	35 (12)	56 (8.1)
c.593C>A (p.Thr198Lys)	26 (10)	11 (1.7)***
c.1087G>T (p.Ala363Ser)	n.d	n.d
c.1402C>G (p.Leu468Val)	56 (13)	62 (8.4)
c.1556G>A (p.Gly519Glu)	31 (13)	45 (7.8)